

Low-rank optimization with trace norm penalty*

B. Mishra[†] G. Meyer[†] F. Bach[‡] R. Sepulchre[†]

October 8, 2018

Abstract

The paper addresses the problem of low-rank trace norm minimization. We propose an algorithm that alternates between fixed-rank optimization and rank-one updates. The fixed-rank optimization is characterized by an efficient factorization that makes the trace norm differentiable in the search space and the computation of duality gap numerically tractable. The search space is nonlinear but is equipped with a particular Riemannian structure that leads to efficient computations. We present a second-order trust-region algorithm with a guaranteed quadratic rate of convergence. Overall, the proposed optimization scheme converges super-linearly to the global solution while still maintaining complexity that is linear in the number of rows of the matrix. To compute a set of solutions efficiently for a grid of regularization parameters we propose a predictor-corrector approach on the quotient manifold that outperforms the naive warm-restart approach. The performance of the proposed algorithm is illustrated on problems of low-rank matrix completion and multivariate linear regression.

1 Introduction

The present paper focuses on the convex program

$$\min_{\mathbf{X} \in \mathbb{R}^{n \times m}} f(\mathbf{X}) + \lambda \|\mathbf{X}\|_* \quad (1)$$

where f is a smooth convex function, $\|\mathbf{X}\|_*$ is the *trace norm* (also known as nuclear norm) which is the sum of the singular values of \mathbf{X} [15, 29, 12] and $\lambda > 0$ is the regularization parameter. Programs of this type have attracted much attention in the recent years as efficient convex relaxations of intractable rank minimization problems [15]. The rank of the optimal solution $\mathbf{X}^*(\lambda)$ of (1) decreases to zero as the regularization parameter grows unbounded [5] and therefore, generating efficiently the regularization path $\{\mathbf{X}^*(\lambda_i)\}_{i=1, \dots, N}$, for a whole range

*This paper presents research results of the Belgian Network DYSCO (Dynamical Systems, Control, and Optimization), funded by the Interuniversity Attraction Poles Programme, initiated by the Belgian State, Science Policy Office. The scientific responsibility rests with its authors.

[†]Department of Electrical Engineering and Computer Science, University of Liège, 4000 Liège, Belgium (B.Mishra@ulg.ac.be, G.Meyer@ulg.ac.be, R.Sepulchre@ulg.ac.be). Bamdev Mishra is a research fellow of the Belgian National Fund for Scientific Research (FNRS).

[‡]INRIA - Sierra Project-Team Ecole Normale Supérieure Paris, France (Francis.Bach@inria.fr)

of values of λ_i minimizers, is a convenient proxy to obtain suboptimal low-rank minimums of f .

Motivated by machine learning and statistical large-scale regression problems [29, 37, 35], we are interested in very low-rank solutions ($p < 10^2$) of very high-dimensional problems ($n > 10^6$). To this end, we propose an algorithm that guarantees second-order convergence to the solutions of (1) while ensuring a tight control (linear in n) on the data storage requirements and on the numerical complexity of each iteration.

The proposed algorithm is based on a low-rank factorization of the unknown matrix, similar to the singular value decomposition (SVD), $\mathbf{X} = \mathbf{U}\mathbf{B}\mathbf{V}^T$. Like in SVD, $\mathbf{U} \in \mathbb{R}^{n \times p}$ and $\mathbf{V} \in \mathbb{R}^{m \times p}$ are orthonormal matrices that span row and column spaces of \mathbf{X} . In contrast, the $p \times p$ scaling factor $\mathbf{B} = \mathbf{B}^T \succ 0$ is allowed to be non-diagonal which makes the factorization non-unique.

Our algorithm alternates between fixed-rank optimization and rank-one updates. When the rank is fixed, the problem is no longer convex but the search space has nevertheless a Riemannian structure. We use the framework of manifold optimization to devise a trust-region algorithm that generates at low-cost (linear in n) iterates that converge super-linearly to a local minimum. Local minima are then escaped by incrementing the rank until the global minimum is reached. The rank-one update is always selected to ensure a decrease of the cost.

Implementing the complete algorithm for a fixed value of the regularization parameter λ leads to a monotone convergence to the global minimum through a sequence of local minima of increasing ranks. Rather, we also modify λ along the way with a predictor-corrector method thereby transforming most local minima of (1) (for fixed λ and fixed rank) into global minima of (1) for different values of λ . The resulting procedure, thus, provides a full regularization path at a very efficient numerical cost.

Not surprisingly, the proposed approach has links with several earlier contributions in the literature. Primarily, the idea of interlacing fixed-rank optimization with rank-one updates has been used in semidefinite programming [11, 17]. It is here extended to a non-symmetric framework using the Riemannian geometry recently developed in [7, 23, 25]. An improvement with respect to earlier work [11, 17] is the use of duality gap certificate to discriminate between local and global minima and its efficient computation thanks to the chosen parametrization.

Schemes that combine manifold optimization and special rank-one updates have appeared recently in the particular context of matrix completion [18, 36]. The framework presented here is in the same spirit but in a more general setting and with a global convergence analysis. Most other fixed-rank algorithms for matrix completion are first-order schemes [32, 18, 22, 30, 36, 23, 8, 34]. It is more difficult to provide a tight comparison of the proposed algorithm to trace norm minimization algorithms that do not fix the rank a priori [12, 21, 37, 4]. It should be emphasized, however, that most trace norm minimization algorithms use singular value thresholding operation at each iteration. This is the most numerically demanding step for these algorithms. For the matrix completion application, it involves computing (potentially all) the singular values of a *low-rank + sparse* matrix. In contrast, the proposed approach only involves rank-one updates. Furthermore, only a few number of such updates are used.

For the sake of illustration and empirical comparison with state-of-the-art algorithms we consider two particular applications, low-rank matrix completion [13] and multivariate linear regression [37]. In both cases, we obtain iterative algorithms with a numerical complexity that is linear in the number of observations and with favorable convergence and precision properties.

2 Relationship between convex program and non-convex formulation

Among the different factorization that exist to represent low-rank matrices, we use the polar factorization [25, 7] that decomposes a p – rank matrix $\mathbf{X} \in \mathbb{R}^{n \times m}$ into

$$\mathbf{X} = \mathbf{U}\mathbf{B}\mathbf{V}^T$$

where $\mathbf{U} \in \text{St}(p, n)$, $\mathbf{V} \in \text{St}(p, m)$ and $\mathbf{B} \in S_{++}(p)$. $\text{St}(p, n)$ is the Stiefel manifold or the set of $n \times p$ matrices with orthonormal columns. $S_{++}(p)$ is the cone of $p \times p$ positive definite matrices. We stress that the scaling $\mathbf{B} = \mathbf{B}^T \succ 0$ is not required to be diagonal. The redundancy of this parametrization has non-trivial algorithmic implications (see Section 3) but we believe that it is key to success of the approach (see [18, 25] for earlier algorithms advocating matrix scaling and Section 6.1 for a numerical illustration). With the use of polar factorization, the trace norm is written as

$$\|\mathbf{X}\|_* = \text{Trace}(\mathbf{B})$$

that makes it differentiable and numerically tractable. The non-convex formulation of (1) is thus recast as

$$\begin{aligned} \min_{\mathbf{U}, \mathbf{B}, \mathbf{V}} \quad & f(\mathbf{U}\mathbf{B}\mathbf{V}^T) + \lambda \text{Trace}(\mathbf{B}) \\ \text{subject to} \quad & \mathbf{U} \in \text{St}(p, n), \quad \mathbf{B} \in S_{++}(p) \quad \text{and} \quad \mathbf{V} \in \text{St}(p, m). \end{aligned} \quad (2)$$

In addition, the search space is not Euclidean but the product space of two well-studied manifolds, namely, the Stiefel manifold [14] and the cone of positive definite matrices [31]. This provides a proper geometric framework to perform optimization. From the geometric point of view, the column and row spaces of \mathbf{X} are represented on the Stiefel manifold whereas the scaling factor is absorbed into the positive definite part. A proper metric on the space takes into account both rotational and scaling invariance. The usefulness of this separation, of subspaces and scaling, has been for instance demonstrated in [18] where the authors use a similar factorization scheme for the matrix completion problem.

2.1 First-order optimality conditions

In order to relate the solution of (2) to that of the convex optimization problem (1) we look at the necessary and sufficient optimality conditions that govern the solutions. The first-order necessary and sufficient optimality condition for the convex program (1) is

$$\mathbf{0} \in \text{Grad}_{\mathbf{X}} f(\mathbf{X}) + \lambda \partial \|\mathbf{X}\|_* \quad (3)$$

where $\text{Grad}_{\mathbf{X}}f$ is the Euclidean gradient of f in $\mathbb{R}^{n \times m}$ at \mathbf{X} and $\partial\|\mathbf{X}\|_*$ is the sub-differential of the trace norm. Details about optimality conditions for trace norm are given in [5, 29]. The first-order necessary conditions (2) are [3, 27, 25]

$$\begin{aligned} \mathbf{S}\mathbf{V}\mathbf{B} - \mathbf{U}\text{Sym}(\mathbf{U}^T\mathbf{S}\mathbf{V}\mathbf{B}) &= \mathbf{0} \\ \text{Sym}(\mathbf{U}^T\mathbf{S}\mathbf{V} + \lambda\mathbf{I}) &= \mathbf{0} \\ \mathbf{S}^T\mathbf{U}\mathbf{B} - \mathbf{V}\text{Sym}(\mathbf{V}^T\mathbf{S}^T\mathbf{U}\mathbf{B}) &= \mathbf{0} \end{aligned} \quad (4)$$

where $\text{Sym}(\mathbf{\Delta}) = \frac{\mathbf{\Delta} + \mathbf{\Delta}^T}{2}$ and $\mathbf{S} = \text{Grad}_{\mathbf{X}}f(\mathbf{U}\mathbf{B}\mathbf{V}^T)$. \mathbf{S} is referred to as *dual variable* throughout the paper. The first-order optimality conditions can be derived either by writing the *Lagrangian* of the problem (2) and looking at the *KKT conditions* or by deriving the gradient of the function on the structured space $\text{St}(p, n) \times S_{++}(p) \times \text{St}(p, m)$ using a metric (11) defined in Section 3.

Proposition 2.1. *A local minimum of (2) $\mathbf{X} = \mathbf{U}\mathbf{B}\mathbf{V}^T$ is also the global optimum of (1) iff*

$$\|\mathbf{S}\|_{op} = \lambda$$

where $\mathbf{S} = \text{Grad}_{\mathbf{X}}f(\mathbf{U}\mathbf{B}\mathbf{V}^T)$ and $\|\mathbf{S}\|_{op}$ is the operator norm, i.e., the dominant singular value of \mathbf{S} . Moreover, $\|\mathbf{S}\|_{op} \geq \lambda$ and equality holds only at optimality.

Proof. This is in fact the first-order optimality condition of (3) [12, 20]. \square

Proposition 2.1 leads to consider the approximate optimality condition that a local minimum of (2) is identified with the global minimum of (1) if $\|\mathbf{S}\|_{op} - \lambda \leq \epsilon$ where ϵ is a user-defined threshold.

2.2 Duality gap computation

Proposition 2.1 provides a criterion to check the global optimality of a solution of (2). However, it provides no guarantees on *closeness* to the global solution. A better way of certifying closeness for the optimization problem of type (1) is provided by the duality gap. The duality gap characterizes the difference of the obtained solution from the optimal solution and is always non-negative [9]. Without loss of generality we introduce a dummy variable $\mathbf{Z} \in \mathbb{R}^{n \times m}$ to rephrase the optimization problem (1) as

$$\begin{aligned} \min_{\mathbf{X}, \mathbf{Z}} \quad & f(\mathbf{X}) + \lambda\|\mathbf{Z}\|_* \\ \text{subject to} \quad & \mathbf{Z} = \mathbf{X}. \end{aligned}$$

The Lagrangian of the problem with dual variable $\mathbf{M} \in \mathbb{R}^{n \times m}$ is written as

$$\mathcal{L}(\mathbf{X}, \mathbf{Z}, \mathbf{M}) = f(\mathbf{X}) + \lambda\|\mathbf{Z}\|_* + \text{Trace}(\mathbf{M}^T(\mathbf{Z} - \mathbf{X}))$$

The *Lagrangian dual* function g of the Lagrangian \mathcal{L} is, then, computed as [9, 6]

$$\begin{aligned} g(\mathbf{M}) &= \min_{\mathbf{X}, \mathbf{Z}} \mathcal{L}(\mathbf{X}, \mathbf{Z}, \mathbf{M}) \\ \implies g(\mathbf{M}) &= \min_{\mathbf{X}, \mathbf{Z}} f(\mathbf{X}) - \text{Trace}(\mathbf{M}^T\mathbf{X}) + \text{Trace}(\mathbf{M}^T\mathbf{Z}) + \lambda\|\mathbf{Z}\|_* \\ \implies g(\mathbf{M}) &= \min_{\mathbf{X}} \{f(\mathbf{X}) - \text{Trace}(\mathbf{M}^T\mathbf{X})\} + \min_{\mathbf{Z}} \{\text{Trace}(\mathbf{M}^T\mathbf{Z}) + \lambda\|\mathbf{Z}\|_*\} \end{aligned}$$

For a pair (\mathbf{X}, \mathbf{M}) the duality gap is then defined as $f(\mathbf{X}) + \lambda\|\mathbf{X}\|_* - g(\mathbf{M})$. To compute the expression of the duality gap we need to calculate analytically g and suggest a value for the dual variable \mathbf{M} . Using the concept of dual norm of trace norm, i.e., operator norm we have

$$\min_{\mathbf{Z}} \text{Trace}(\mathbf{M}^T \mathbf{Z}) + \lambda\|\mathbf{Z}\|_* = 0 \quad \text{if} \quad \|\mathbf{M}\|_{op} \leq \lambda$$

Similarly, using the concept of Fenchel conjugate of a function we have

$$\min_{\mathbf{X}} f(\mathbf{X}) - \text{Trace}(\mathbf{M}^T \mathbf{X}) = -f^*(\mathbf{M})$$

where f^* is the Fenchel conjugate [6, 9] of f , defined as

$$f^*(\mathbf{M}) = \sup_{\mathbf{X} \in \mathbb{R}^{n \times m}} [\text{Trace}(\mathbf{M}^T \mathbf{X}) - f(\mathbf{X})].$$

The final expression for the dual function is, thus, [6]

$$g(\mathbf{M}) = -f^*(\mathbf{M}) \quad \text{subject to} \quad \|\mathbf{M}\|_{op} \leq \lambda.$$

The final expression of duality gap is

$$f(\mathbf{X}) + \lambda\|\mathbf{X}\|_* - g(\mathbf{M}) = f(\mathbf{X}) + \lambda\|\mathbf{X}\|_* + f^*(\mathbf{M}) \quad \text{subject to} \quad \|\mathbf{M}\|_{op} \leq \lambda \quad (5)$$

where \mathbf{M} is the *dual candidate*. A good choice for the dual candidate \mathbf{M} is \mathbf{S} ($= \text{Grad}_{\mathbf{X}} f(\mathbf{X})$) with appropriate scaling to satisfy the operator norm constraint: $\mathbf{M} = \min\{1, \frac{\lambda}{\|\mathbf{S}\|_{op}}\} \mathbf{S}$ [6].

As an extension for some functions f of type $f(\mathbf{X}) = \psi(\mathcal{A}(\mathbf{X}))$ where \mathcal{A} is a linear operator, computing the Fenchel conjugate of the function ψ may be easier than that of f . The duality gap, using similar calculations as above, is obtained as

$$f(\mathbf{X}) + \lambda\|\mathbf{X}\|_* + \psi^*(\mathbf{M}) \quad \text{subject to} \quad \|\mathcal{A}^*(\mathbf{M})\|_{op} \leq \lambda$$

where \mathcal{A}^* is the adjoint operator of \mathcal{A} and ψ^* is the Fenchel conjugate of ψ . A good choice of \mathbf{M} is again $\min\{1, \frac{\lambda}{\sigma_\psi}\} \text{Grad} \psi$ where σ_ψ is the dominant singular value of $\mathcal{A}^*(\text{Grad} \psi)$ [6].

3 Manifold-based optimization to solve the non-convex problem (2)

In this section we solve the problem (2) to obtain a local minimum. In contrast to first-order optimization algorithms proposed earlier in [25, 24, 18], we develop a second-order trust-region algorithm that has a quadratic rate of convergence [27, 3]. The idea behind a trust-region algorithm is to build locally a quadratic model of the function at a point and solve the *trust-region subproblem* to get the next potential iterate. Depending on whether the decrease in the objective function is sufficient or not, the potential iterate is accepted or rejected. Details about a general trust-region algorithm are given in [27]. Rewriting the problem (2) as

$$\begin{aligned} \min_{\mathbf{U}, \mathbf{B}, \mathbf{V}} \quad & \bar{\phi}(\mathbf{U}, \mathbf{B}, \mathbf{V}) \\ \text{subject to} \quad & (\mathbf{U}, \mathbf{B}, \mathbf{V}) \in \text{St}(p, n) \times S_{++}(p) \times \text{St}(p, m) \end{aligned} \quad (6)$$

where $\bar{\phi}(\mathbf{U}, \mathbf{B}, \mathbf{V}) = f(\mathbf{UBV}^T) + \lambda \text{Trace}(\mathbf{B})$ is introduced for notational convenience. An important observation for second-order algorithms [2, 3] is that the local minima of the problem (6) are not isolated in the search space

$$\overline{\mathcal{M}}_p = \text{St}(p, n) \times S_{++}(p) \times \text{St}(p, m).$$

This is because the cost function is invariant under rotations, i.e.,

$$\mathbf{UBV}^T = (\mathbf{UO})(\mathbf{O}^T\mathbf{BO})(\mathbf{VO})^T$$

for any $p \times p$ rotation matrix $\mathbf{O} \in \mathcal{O}(p)$. To remove the symmetry of the cost function, we identify all the points of the search space that belong to the equivalence class defined by

$$[(\mathbf{U}, \mathbf{B}, \mathbf{V})] = \{(\mathbf{UO}, \mathbf{O}^T\mathbf{BO}, \mathbf{VO}) | \mathbf{O} \in \mathcal{O}(p)\}.$$

The set of all such equivalence classes is termed the quotient manifold of $\overline{\mathcal{M}}_p$ by $\mathcal{O}(p)$, i.e., denoted by

$$\mathcal{M}_p = \overline{\mathcal{M}}_p / \mathcal{O}(p). \quad (7)$$

The problem (6) is thus conceptually an *unconstrained* optimization problem on the quotient manifold \mathcal{M}_p in which the minima are isolated. Computations are performed in the total space $\overline{\mathcal{M}}_p$, which is the product space of well-studied manifolds.

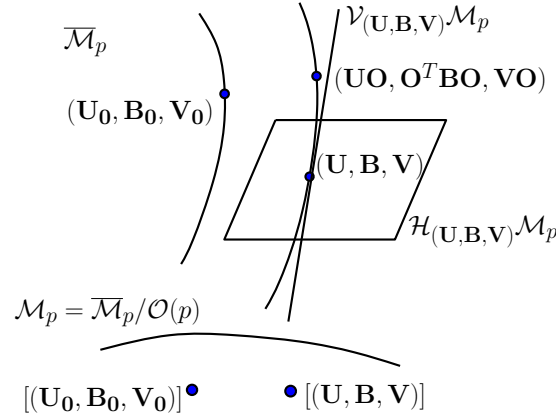


Figure 1: The quotient manifold representation of the search space.

Tangent space of \mathcal{M}_p

Tangent vectors at a point $x \in \mathcal{M}_p$ have a matrix representation in the tangent space of the total space $\overline{\mathcal{M}}_p$. Note that \bar{x} belongs to $\overline{\mathcal{M}}_p$ and its equivalence class is represented by the element $x \in \mathcal{M}_p$ such that $x = [\bar{x}]$. Because the total space is a product space $\text{St}(p, n) \times S_{++}(p) \times \text{St}(p, m)$, its tangent space admits the decomposition at a point $\bar{x} = (\mathbf{U}, \mathbf{B}, \mathbf{V})$

$$T_{\bar{x}}\overline{\mathcal{M}}_p = T_{\mathbf{U}}\text{St}(p, n) \times T_{\mathbf{B}}S_{++}(p) \times T_{\mathbf{V}}\text{St}(p, m)$$

and the following characterizations are well-known [14, 31]

$$\begin{aligned} T_{\mathbf{U}}\text{St}(p, n) &= \{\mathbf{U}\boldsymbol{\Omega} + \mathbf{U}_{\perp}\mathbf{K} \mid \boldsymbol{\Omega} \in S_{skew}(p), \mathbf{K} \in \mathbb{R}^{(n-p) \times p}\} \\ &= \{\mathbf{Z}_{\mathbf{U}} - \mathbf{U}\text{Sym}(\mathbf{U}^T \mathbf{Z}_{\mathbf{U}}) \mid \mathbf{Z}_{\mathbf{U}} \in \mathbb{R}^{n \times p}\} \\ T_{\mathbf{B}}S_{++}(p) &= S_{sym}(p) \end{aligned}$$

where $S_{sym}(p)$ is the set of $p \times p$ symmetric matrices, $S_{skew}(p)$ is the set of $p \times p$ skew-symmetric matrices and \mathbf{U}_{\perp} is the orthogonal complement of the space spanned by \mathbf{U} . Note that an arbitrary matrix $(\mathbf{Z}_{\mathbf{U}}, \mathbf{Z}_{\mathbf{B}}, \mathbf{Z}_{\mathbf{V}}) \in \mathbb{R}^{n \times p} \times \mathbb{R}^{p \times p} \times \mathbb{R}^{m \times (p)}$ is projected on the tangent space $T_{\bar{x}}\overline{\mathcal{M}}_p$ by the linear operation

$$\Psi_{\bar{x}}(\mathbf{Z}_{\mathbf{U}}, \mathbf{Z}_{\mathbf{B}}, \mathbf{Z}_{\mathbf{V}}) = (\mathbf{Z}_{\mathbf{U}} - \mathbf{U}\text{Sym}(\mathbf{U}^T \mathbf{Z}_{\mathbf{U}}), \text{Sym}(\mathbf{Z}_{\mathbf{B}}), \mathbf{Z}_{\mathbf{V}} - \mathbf{V}\text{Sym}(\mathbf{V}^T \mathbf{Z}_{\mathbf{V}})). \quad (8)$$

A matrix representation of the tangent space at $x \in \mathcal{M}_p$ relies on the decomposition of $T_{\bar{x}}\overline{\mathcal{M}}_p$ into its *vertical* and *horizontal* subspaces. The vertical space $\mathcal{V}_{\bar{x}}\mathcal{M}_p$ is the subspace of $T_{\bar{x}}\overline{\mathcal{M}}_p$ that is tangent to the equivalence class $[\bar{x}]$

$$\mathcal{V}_{\bar{x}}\mathcal{M}_p = \{(\mathbf{U}\boldsymbol{\Omega}, \mathbf{B}\boldsymbol{\Omega} - \boldsymbol{\Omega}\mathbf{B}, \mathbf{V}\boldsymbol{\Omega}) \mid \boldsymbol{\Omega} \in S_{skew}(p)\}. \quad (9)$$

The horizontal space $\mathcal{H}_{\bar{x}}\mathcal{M}_p$ must be chosen such that

$$T_{\bar{x}}\overline{\mathcal{M}}_p = \mathcal{H}_{\bar{x}}\mathcal{M}_p \oplus \mathcal{V}_{\bar{x}}\mathcal{M}_p. \quad (10)$$

We choose $\mathcal{H}_{\bar{x}}\mathcal{M}_p$ as the orthogonal complement of $\mathcal{V}_{\bar{x}}\mathcal{M}_p$ for the metric

$$\begin{aligned} \bar{g}_{\bar{x}}(\xi_{\bar{x}}, \eta_{\bar{x}}) &= \text{Trace}(\xi_{\mathbf{U}}^T \eta_{\mathbf{U}}) + \text{Trace}(\mathbf{B}^{-1} \xi_{\mathbf{B}} \mathbf{B}^{-1} \eta_{\mathbf{B}}) \\ &\quad + \text{Trace}(\xi_{\mathbf{V}}^T \eta_{\mathbf{V}}), \end{aligned} \quad (11)$$

which picks the normal metric of the Stiefel manifold [14] and the natural metric of the positive definite cone [31]. Here $\xi_{\bar{x}}$ and $\eta_{\bar{x}}$ are elements of $T_{\bar{x}}\mathcal{M}_p$. With this choice, a horizontal tangent vector $\zeta_{\bar{x}}$ is any tangent vector $(\zeta_{\mathbf{U}}, \zeta_{\mathbf{B}}, \zeta_{\mathbf{V}})$ belonging to the set

$$\mathcal{H}_{\bar{x}}\mathcal{M}_p = \{(\zeta_{\mathbf{U}}, \zeta_{\mathbf{B}}, \zeta_{\mathbf{V}}) \in T_{\bar{x}}\overline{\mathcal{M}}_p \mid \bar{g}_{\bar{x}}((\zeta_{\mathbf{U}}, \zeta_{\mathbf{B}}, \zeta_{\mathbf{V}}), (\mathbf{U}\boldsymbol{\Omega}, (\mathbf{B}\boldsymbol{\Omega} - \boldsymbol{\Omega}\mathbf{B}), \mathbf{V}\boldsymbol{\Omega})) = 0\} \quad (12)$$

Starting from an arbitrary tangent vector $\eta_{\bar{x}} \in T_{\bar{x}}\overline{\mathcal{M}}_p$ we construct its projection on the horizontal space by picking $\boldsymbol{\Omega} \in S_{skew}(p)$ such that

$$\Pi_{\bar{x}}(\eta_{\bar{x}}) = (\eta_{\mathbf{U}} - \mathbf{U}\boldsymbol{\Omega}, \eta_{\mathbf{B}} - (\mathbf{B}\boldsymbol{\Omega} - \boldsymbol{\Omega}\mathbf{B}), \eta_{\mathbf{V}} - \mathbf{V}\boldsymbol{\Omega}) \in \mathcal{H}_{\bar{x}}\mathcal{M}_p, \quad (13)$$

Using the calculation (12), the unique $\boldsymbol{\Omega}$ that satisfies (13) is the solution of the *Sylvester* equation

$$\boldsymbol{\Omega}\mathbf{B}^2 + \mathbf{B}^2\boldsymbol{\Omega} = \mathbf{B}(\text{Skew}(\mathbf{U}^T \eta_{\mathbf{U}}) - 2\text{Skew}(\mathbf{B}^{-1} \eta_{\mathbf{B}}) + \text{Skew}(\mathbf{V}^T \eta_{\mathbf{V}}))\mathbf{B} \quad (14)$$

where $\text{Skew}(\mathbf{A}) = \frac{\mathbf{A} - \mathbf{A}^T}{2}$. The numerical complexity of solving the Sylvester equation is $O(p^3)$.

The Riemannian submersion (\mathcal{M}_p, g)

The choice of the metric (11), which is invariant along the equivalence class $[\bar{x}]$, and of the horizontal space (12) turn the quotient manifold \mathcal{M}_p into a Riemannian submersion of $(\overline{\mathcal{M}}_p, \bar{g})$ [3]. As shown in [3], this special construction allows for a convenient matrix representation of the gradient and the Hessian on the abstract manifold \mathcal{M}_p . The Riemannian gradient of $\phi : \mathcal{M}_p \rightarrow \mathbb{R} : x \mapsto \phi(x) = \bar{\phi}(\bar{x})$ is uniquely represented by its horizontal lift in $\overline{\mathcal{M}}_p$ which has the matrix representation

$$\overline{\text{grad}_x \phi} = \Pi_{\bar{x}}(\text{grad}_{\bar{x}} \bar{\phi}).$$

On the other hand, the matrix expression of $\text{grad}_x \bar{\phi}$ at a point $\bar{x} = (\mathbf{U}, \mathbf{B}, \mathbf{V})$ is standard: the Euclidean gradient $(\text{Grad}_{\mathbf{U}} \bar{\phi}, \text{Grad}_{\mathbf{B}} \bar{\phi}, \text{Grad}_{\mathbf{V}} \bar{\phi})$ must simply be projected on $T_{\bar{x}} \overline{\mathcal{M}}_p$, i.e.,

$$\text{grad}_{\bar{x}} \bar{\phi} = \Psi_{\bar{x}}(\text{Grad}_{\mathbf{U}} \bar{\phi}, \text{Grad}_{\mathbf{B}} \bar{\phi}, \text{Grad}_{\mathbf{V}} \bar{\phi})$$

Likewise, the Riemannian connection $\nabla_\nu \eta$ on \mathcal{M}_p is uniquely represented by its horizontal lift in $\overline{\mathcal{M}}_p$ which is

$$\overline{\nabla_\nu \eta} = \Pi_{\bar{x}}(\overline{\nabla_{\bar{\nu}} \bar{\eta}}).$$

where ν and η are vector fields in \mathcal{M}_p and $\bar{\nu}$ and $\bar{\eta}$ are their horizontal lifts in $\overline{\mathcal{M}}_p$. Once again, the Riemannian connection $\overline{\nabla_{\bar{\nu}} \bar{\eta}}$ on $\overline{\mathcal{M}}_p$ has well-known expression [16, 31, 3], obtained by means of the *Koszul formula*, given by

$$\overline{\nabla_{\bar{\nu}} \bar{\eta}} = \Psi_{\bar{x}}(D\bar{\eta}[\bar{\nu}]) - \Psi_{\bar{x}} \left(\nu_{\mathbf{U}} \text{Sym}(\mathbf{U}^T \eta_{\mathbf{U}}), \text{Sym}(\nu_{\mathbf{B}} \mathbf{B}^{-1} \eta_{\mathbf{B}}), \nu_{\mathbf{V}} \text{Sym}(\mathbf{V}^T \eta_{\mathbf{V}}) \right). \quad (15)$$

Here $D\bar{\eta}[\bar{\nu}]$ is the classical Euclidean directional derivative of $\bar{\eta}$ in the direction $\bar{\nu}$. The Riemannian Hessian in $\overline{\mathcal{M}}_p$ has, thus, the following matrix expression

$$\overline{\text{Hess} \phi(x)[\xi]} = \Pi_{\bar{x}}(\overline{\nabla_{\bar{\xi}} \text{grad} \bar{\phi}}). \quad (16)$$

for any $\xi \in T_x \mathcal{M}_p$ and its horizontal lift $\bar{\xi} \in \mathcal{H}_{\bar{x}} \overline{\mathcal{M}}_p$.

Trust-region subproblem and retraction on \mathcal{M}_p

Analogous to trust-region algorithms in the Euclidean space, trust-region algorithms on a quotient manifold with guaranteed quadratic rate convergence have been proposed in [1, 3]. The trust-region subproblem on \mathcal{M} is formulated as

$$\begin{aligned} \min_{\xi \in T_x \mathcal{M}_p} \quad & \phi(x) + g_x(\xi, \text{grad} \phi(x)) + \frac{1}{2} g_x(\xi, \text{Hess} \phi(x)[\xi]) \\ \text{subject to} \quad & g_x(\xi, \xi) \leq \delta. \end{aligned}$$

where δ is the trust-region radius and $\text{grad} \phi$ and $\text{Hess} \phi$ are the Riemannian gradient and Hessian on \mathcal{M}_p . The problem is horizontally lifted to the horizontal space $\mathcal{H}_{\bar{x}} \overline{\mathcal{M}}_p$ where it is solved using a *truncated-conjugate gradient* method with parameters set as in Alg. 2 of [1]. Refer [1] for further details. Solving the above trust-region subproblem leads to a direction ξ that minimizes the quadratic model. To find the new iterate based on the obtained direction ξ , a mapping from the tangent space $T_x \mathcal{M}_p$ to the manifold \mathcal{M}_p is required. This mapping

is more generally referred to as *retraction* which maps the vectors from the tangent space onto the points on the manifold, $R_x : T_x \mathcal{M}_p \rightarrow \mathcal{M}_p$ (details in [3]). In the present case, a retraction of interest is [3, 25]

$$\begin{aligned} R_{\mathbf{U}}(\xi_{\mathbf{U}}) &= \text{uf}(\mathbf{U} + \xi_{\mathbf{U}}) \\ R_{\mathbf{B}}(\xi_{\mathbf{B}}) &= \mathbf{B}^{\frac{1}{2}} \exp(\mathbf{B}^{-\frac{1}{2}} \xi_{\mathbf{B}} \mathbf{B}^{-\frac{1}{2}}) \mathbf{B}^{\frac{1}{2}} \\ R_{\mathbf{V}}(\xi_{\mathbf{V}}) &= \text{uf}(\mathbf{V} + \xi_{\mathbf{V}}) \end{aligned} \quad (17)$$

where uf is a function that extracts the orthogonal factor of the polar factorization and \exp is the *matrix exponential* operator. The retraction on the positive definite cone is the natural exponential mapping for the metric (11) [31].

Numerical complexity

The numerical complexity per iteration of the proposed trust-region algorithm to solve (6) depends on the computational cost of the following components.

- Objective function $\bar{\phi} \rightarrow$ problem dependent
- Metric $\bar{g} \rightarrow O(np^2 + mp^2 + p^3)$
- Euclidean gradient of $\bar{\phi} \rightarrow$ problem dependent
- $\bar{\nabla}_{\bar{\nu}} \bar{\eta} = \Psi(\text{D}\bar{\eta}[\bar{\nu}]) - \Psi(\nu_{\mathbf{U}} \text{Sym}(\mathbf{U}^T \eta_{\mathbf{U}}), \text{Sym}(\nu_{\mathbf{B}} \mathbf{B}^{-1} \eta_{\mathbf{B}}), \nu_{\mathbf{V}} \text{Sym}(\mathbf{V}^T \eta_{\mathbf{V}}))$
 - $\text{D}\bar{\eta}[\bar{\nu}] \rightarrow$ problem dependent
 - Matrix $\nu_{\mathbf{U}} \text{Sym}(\mathbf{U}^T \eta_{\mathbf{U}}) \rightarrow O(np^2)$
 - Matrix $\text{Sym}(\nu_{\mathbf{B}} \mathbf{B}^{-1} \eta_{\mathbf{B}}) \rightarrow O(p^3)$
 - Matrix $\nu_{\mathbf{V}} \text{Sym}(\mathbf{V}^T \eta_{\mathbf{V}}) \rightarrow O(mp^2)$
- Projection operator $\Psi \rightarrow O(np^2 + mp^2)$
- Projection operator $\Pi \rightarrow O(np^2 + mp^2 + p^3)$
 - Sylvester equation for $\mathbf{\Omega} \rightarrow O(p^3)$
- Retraction $R \rightarrow O(np^2 + mp^2 + p^3)$

As shown above all the manifold related operations are of linear complexity in n and m . Other operations depend on the problem at hand and are computed in the search space $\overline{\mathcal{M}}_p$. With $p \ll \min\{n, m\}$ the computational burden on the algorithm considerably reduces. Similarly, sparsity in the problem can also be exploited to compute the components “cheaply”.

4 An optimization scheme to solve convex program (1)

In order to solve the convex program (1), we alternate a second-order local optimization algorithm on fixed-rank manifold with a first-order rank-one update. The scheme is shown in Table 1. The rank update is constructed in such a way that

Algorithm to solve convex problem (1)

0.
 - Initialize p to p_0 , a guess rank.
 - Initialize the threshold ϵ for convergence criterion, refer to Proposition 2.1.
 - Initialize the iterates $\mathbf{U}_0 \in \text{St}(p_0, n)$, $\mathbf{B}_0 \in S_{++}(p_0)$ and $\mathbf{V}_0 \in \text{St}(p_0, m)$.
1. Solve the non-convex problem (2) in the dimension p to obtain a local minimum $(\mathbf{U}, \mathbf{B}, \mathbf{V})$.
2. Compute σ_1 (the dominant singular value) of dual variable $\mathbf{S} = \text{Grad}_{\mathbf{X}} f(\mathbf{UBV}^T)$.
 - If $\sigma_1 - \lambda \leq \epsilon$ (or duality gap $\leq \epsilon$), output $\mathbf{X} = \mathbf{UBV}^T$ as the solution to problem (1) and stop.
 - Else, compute the update as shown in Theorem (4.1) and compute the new point $(\mathbf{U}_+, \mathbf{B}_+, \mathbf{V}_+)$ as described in (19). Set $p = p + 1$ and repeat step 1.

Table 1: Algorithm to solve the trace norm minimization problem of type (1).

1. it ensures a descent property of the cost and
2. it maps a point $(\mathbf{U}, \mathbf{B}, \mathbf{V}) \in \overline{\mathcal{M}}_p$ to $(\mathbf{U}_+, \mathbf{B}_+, \mathbf{V}_+) \in \overline{\mathcal{M}}_{p+1}$.

Proposition 4.1. *If $\mathbf{X} = \mathbf{UBV}^T$ then the rank-one update*

$$\mathbf{X}_+ = \mathbf{X} - \beta uv^T \quad (18)$$

ensures a decrease in the objective function $f(\mathbf{X}) + \lambda \|\mathbf{X}\|_$ provided that $\beta > 0$ is sufficiently small and the descent directions $u \in \mathbb{R}^n$ and $v \in \mathbb{R}^m$ are chosen as the dominant left and right singular vectors of the dual variable $\mathbf{S} = \text{Grad}_{\mathbf{X}} f(\mathbf{UBV}^T)$.*

Proof. This is in fact a descent step as shown in [12, 20, 21] but now projected onto the rank-one dominant subspace. \square

A representation of \mathbf{X}_+ on $\overline{\mathcal{M}}_{p+1}$ is obtained from the singular value decomposition of \mathbf{X}_+ . Since \mathbf{X}_+ is a rank-one update of \mathbf{UBV}^T , the singular value decomposition can be performed efficiently [10]. Defining u' and v' such that $u' = (\mathbf{I} - \mathbf{UU}^T)u$ and $v' = (\mathbf{I} - \mathbf{VV}^T)(-\beta v)$, which are the orthogonal projections of u and v on the complementary space of \mathbf{U} and \mathbf{V} , the update (18) is written as

$$\begin{aligned} \mathbf{X}_+ &= \mathbf{UBV}^T - \beta uv^T = [\mathbf{U} \quad u] \begin{bmatrix} \mathbf{B} & \mathbf{0} \\ \mathbf{0} & 1 \end{bmatrix} [\mathbf{V} \quad -\beta v]^T \\ &= [\mathbf{U} \quad \frac{u'}{\|u'\|}] \mathbf{K} [\mathbf{V} \quad \frac{v'}{\|v'\|}]^T \end{aligned}$$

where

$$\mathbf{K} = \begin{bmatrix} 1 & \mathbf{U}^T u \\ \mathbf{0} & \|u'\| \end{bmatrix} \begin{bmatrix} \mathbf{B} & \mathbf{0} \\ \mathbf{0} & 1 \end{bmatrix} \begin{bmatrix} 1 & -\beta \mathbf{V}^T v \\ \mathbf{0} & 1 \end{bmatrix}^T.$$

It should be noted that \mathbf{K} is of size $(p + 1) \times (p + 1)$. If $\mathbf{P}'\boldsymbol{\Sigma}'\mathbf{Q}'^T$ is the singular value decomposition of \mathbf{K} where \mathbf{P}' and \mathbf{Q}' are orthonormal matrices and $\boldsymbol{\Sigma}'$ is a diagonal matrix then the new point $\mathbf{X}_+ \in \overline{\mathcal{M}}_{p+1}$ is given by

$$\mathbf{U}_+ = [\mathbf{U} \quad \frac{u'}{\|u'\|}]\mathbf{P}', \quad \mathbf{B}_+ = \boldsymbol{\Sigma}' \quad \text{and} \quad \mathbf{V}_+ = [\mathbf{V} \quad \frac{v'}{\|v'\|}]\mathbf{Q}'. \quad (19)$$

To compute β we perform a *backtracking* line search.

Comments

The algorithm described in Table 1 always converges to the global solution and stops at most when $p = \min\{m, n\}$. In this case we end up solving the original problem itself. However, in practice the algorithm stops at a rank $p \ll \min\{m, n\}$ (often $p = r$ where r is the optimal rank) as clear from the numerical experiments presented later in section (6). This makes it appealing for large-scale applications where memory requirements are a major issue, e.g., [17, 26, 25]. One advantage of the scheme, in contrast to trace norm minimization algorithms proposed in [12, 33, 20, 21], is that it offers a tight control of the rank at all intermediate iterates of the scheme. In singular value thresholding schemes, for each iteration, the (full) Euclidean gradient information is proposed necessary for the singular value shrinkage operation [12] that thresholds the rank. In contrast, our scheme uses only rank-one information of the gradient while incrementing rank and a rank- p information while optimizing on the fixed-rank manifold.

Another advantage is that the stopping criterion threshold of the non-convex (2) and that of the convex (1) can be separated. This means that rank-increments can be made after a fixed number of iterations of the manifold optimization without waiting for the trust-region algorithm to converge to a local minimum.

5 Regularization path

In applications the optimal value of λ is usually unknown [21] and hence, there is a need to solve (1) for a number of regularization parameters. In addition, even if the optimal λ is a priori known, it might be better to build a path of solutions corresponding to different values of λ that lead to the optimal value. This gives more interpretability to the intermediate iterates which are now seen as global minima for different values of λ . This motivates the interest in an efficient way to compute the full solution (or regularization) path of (1) for a number of values λ , i.e., defined as

$$\mathbf{X}^*(\lambda_i) = \arg \min_{\mathbf{X} \in \mathbb{R}^{n \times m}} f(\mathbf{X}) + \lambda_i \|\mathbf{X}\|_*$$

where $\mathbf{X}^*(\lambda_i)$ is the solution to the λ_i minimization problem. A common approach is the *warm-restart* approach where the algorithm to solve the λ_{i+1} problem is initialized from $\mathbf{X}^*(\lambda_i)$ and so on [21]. However, the warm-restart approach does not utilize the fact that the regularization path is often (to some degree) *smooth* especially when the values of λ are close to each other. In this section we describe a *predictor-corrector* scheme that takes into account the first-order smoothness and computes the path efficiently. To compute the path

Computing the regularization path

0. Given $\{\lambda_i\}_{i=1,\dots,N}$ in decreasing order. Also given are the solutions $\mathbf{X}^*(\lambda_1)$ and $\mathbf{X}^*(\lambda_2)$ at λ_1 and λ_2 respectively and their low-rank factorizations.
1. Predictor step:
 - If $\mathbf{X}^*(\lambda_{i-1})$ and $\mathbf{X}^*(\lambda_i)$ belong to the same quotient manifold \mathcal{M}_p then construct a first-order approximation of the solution path at λ_i and estimate $\hat{\mathbf{X}}(\lambda_{i+1})$ as shown in (21).
 - Else $\hat{\mathbf{X}}(\lambda_{i+1}) = \mathbf{X}^*(\lambda_i)$.
2. Corrector step: Using the estimated solution of the λ_{i+1} – problem, initialize the algorithm described in Table 1 to compute the exact solution $\mathbf{X}^*(\lambda_{i+1})$.
3. Repeat steps 1 and 2 for all subsequent values of λ .

Table 2: Algorithm for computing the regularization path. If N is the number of values of λ and r is the number of rank increments then the scheme uses r warm restarts and $N - r$ predictor steps to compute the full path.

we take a *predictor* (estimator) step to predict the solution and then rectify the prediction by a *corrector* step. This scheme has been widely used in solving differential equations and regression problems [28]. We extend the *prediction* idea to the quotient manifold \mathcal{M}_p . The corrector step is carried out by initializing the algorithm in Table 1 from the predicted point. If $\mathbf{X}^*(\lambda_i) = \mathbf{U}_i \mathbf{B}_i \mathbf{V}_i^T$ is the polar factorization then the solution of the λ_{i+1} optimization problem is predicted (or estimated), i.e., $\hat{\mathbf{X}}(\lambda_{i+1}) = \hat{\mathbf{U}}_{i+1} \hat{\mathbf{B}}_{i+1} \hat{\mathbf{V}}_{i+1}^T$, by the two previous solutions $\mathbf{X}^*(\lambda_i)$ and $\mathbf{X}^*(\lambda_{i-1})$ at λ_i and λ_{i-1} respectively belonging to the same rank manifold \mathcal{M}_p . When $\mathbf{X}^*(\lambda_{i-1})$ and $\mathbf{X}^*(\lambda_i)$ belong to different rank manifolds we perform instead a warm restart to solve λ_{i+1} problem. The complete scheme is shown in Table 2 and has the following advantages.

- With a few number of rank increments we traverse the entire path.
- Potentially every iterate of the optimization scheme is now a global solution for a value of λ .
- The predictor-corrector approach outperforms the warm-restart approach in maximizing *prediction accuracy* with minimal extra computations.

In this section, we assume that the optimization problem (1) has a unique solution for all λ . A sufficient condition is that f is strictly convex, which can be enforced by adding a small multiple of the square Frobenius norm to f .

Predictor step on the quotient manifold \mathcal{M}_p

Assuming (first-order) smoothness of the regularization path on \mathcal{M}_p connecting $(\mathbf{U}_i, \mathbf{B}_i, \mathbf{V}_i)$ and $(\mathbf{U}_{i-1}, \mathbf{B}_{i-1}, \mathbf{V}_{i-1})$ in $\overline{\mathcal{M}}_p$, we build a first-order approximation of the geodesic, i.e. the curve of shortest length, connecting the two points. The estimated solution $\hat{\mathbf{X}}(\lambda_{i+1})$

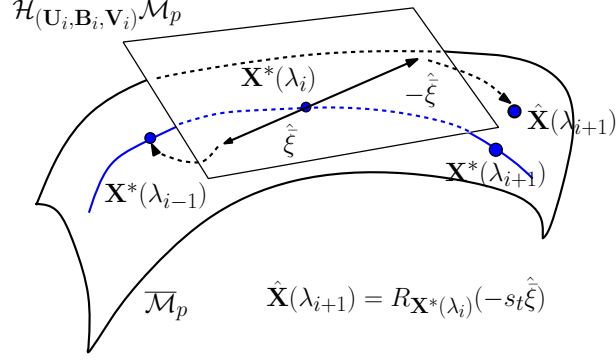


Figure 2: Tracing the path of solutions using predictor-corrector approach. The blue line denotes the curve of optimal solutions.

is then computed by extending the geodesic. In other words, we need to identify a vector $\xi \in T_{[(\mathbf{U}_i, \mathbf{B}_i, \mathbf{V}_i)]} \mathcal{M}_p$ and its horizontal lift $\bar{\xi} \in \mathcal{H}_{(\mathbf{U}_i, \mathbf{B}_i, \mathbf{V}_i)} \mathcal{M}_p$ at $(\mathbf{U}_i, \mathbf{B}_i, \mathbf{V}_i)$ on $\bar{\mathcal{M}}_p$ defined as

$$\bar{\xi} = \text{Log}_{(\mathbf{U}_i, \mathbf{B}_i, \mathbf{V}_i)}(\mathbf{U}_{i-1}, \mathbf{B}_{i-1}, \mathbf{V}_{i-1})$$

that maps $(\mathbf{U}_{i-1}, \mathbf{B}_{i-1}, \mathbf{V}_{i-1})$ on $\bar{\mathcal{M}}_p$ to the horizontal space $\mathcal{H}_{(\mathbf{U}_j, \mathbf{B}_j, \mathbf{V}_j)} \mathcal{M}_p$ [3]. Log is referred to as *logarithmic mapping*. Computing the logarithmic mapping (and hence, the geodesic) might be numerically costly in general. For the case of interest there is no analytic expression for the logarithmic mapping. Instead a numerically efficient way is to use the inverse retraction $R_{(\mathbf{U}_i, \mathbf{B}_i, \mathbf{V}_i)}^{-1}(\mathbf{U}_{i-1}, \mathbf{B}_{i-1}, \mathbf{V}_{i-1})$ where $R^{-1} : \bar{\mathcal{M}}_p \rightarrow \mathcal{E}$ to obtain a direction in the space \mathcal{E} followed by *projection* onto the horizontal space $\mathcal{H}_{(\mathbf{U}_j, \mathbf{B}_j, \mathbf{V}_j)} \mathcal{M}_p$. Note that $\mathcal{E} := \mathbb{R}^{n \times p} \times \mathbb{R}^{p \times p} \times \mathbb{R}^{m \times p}$. The projection is accomplished using projection operators $\Psi : \mathcal{E} \rightarrow T_{(\mathbf{U}_i, \mathbf{B}_i, \mathbf{V}_i)} \bar{\mathcal{M}}_p$ and $\Pi : T_{(\mathbf{U}_i, \mathbf{B}_i, \mathbf{V}_i)} \bar{\mathcal{M}}_p \rightarrow \mathcal{H}_{(\mathbf{U}_i, \mathbf{B}_i, \mathbf{V}_i)} \mathcal{M}_p$ defined in Section 3. Hence, an estimate on $\bar{\xi}$ is given as

$$\hat{\xi} = \Pi(\Psi(R_{(\mathbf{U}_i, \mathbf{B}_i, \mathbf{V}_i)}^{-1}(\mathbf{U}_{i-1}, \mathbf{B}_{i-1}, \mathbf{V}_{i-1}))) \quad (20)$$

For the retraction of interest (17) the *Frobenius norm* error in the approximation of the Logarithmic mapping is bounded as

$$\begin{aligned} \|\hat{\xi} - \bar{\xi}\|_F &= \|\hat{\xi} - R_{(\mathbf{U}_i, \mathbf{B}_i, \mathbf{V}_i)}^{-1}(\mathbf{U}_{i-1}, \mathbf{B}_{i-1}, \mathbf{V}_{i-1}) + R_{(\mathbf{U}_i, \mathbf{B}_i, \mathbf{V}_i)}^{-1}(\mathbf{U}_{i-1}, \mathbf{B}_{i-1}, \mathbf{V}_{i-1}) - \bar{\xi}\|_F \\ &\leq \|\hat{\xi} - R_{(\mathbf{U}_i, \mathbf{B}_i, \mathbf{V}_i)}^{-1}(\mathbf{U}_{i-1}, \mathbf{B}_{i-1}, \mathbf{V}_{i-1})\|_F + \|R_{(\mathbf{U}_i, \mathbf{B}_i, \mathbf{V}_i)}^{-1}(\mathbf{U}_{i-1}, \mathbf{B}_{i-1}, \mathbf{V}_{i-1}) - \bar{\xi}\|_F \\ &\leq \min_{\bar{\zeta} \in \mathcal{H}_{(\mathbf{U}_i, \mathbf{B}_i, \mathbf{V}_i)} \mathcal{M}_p} \|\bar{\zeta} - R_{(\mathbf{U}_i, \mathbf{B}_i, \mathbf{V}_i)}^{-1}(\mathbf{U}_{i-1}, \mathbf{B}_{i-1}, \mathbf{V}_{i-1})\|_F + O(\|\bar{\xi}\|_F^2), \\ &\quad \text{as } \|\bar{\xi}\| \rightarrow 0. \end{aligned}$$

The $O(\|\bar{\xi}\|_F^2)$ approximation error comes from the fact that the retraction R used is a first-order retraction [3]. This approximation is exact if $\bar{\mathcal{M}}_p$ is the Euclidean space. The inverse retraction corresponding to the retraction R described in (17) is computed as

$$\begin{aligned} R_{\mathbf{U}_i}^{-1}(\mathbf{U}_{i-1}) &= \mathbf{U}_{i-1} - \mathbf{U}_i \\ R_{\mathbf{B}_i}^{-1}(\mathbf{B}_{i-1}) &= \mathbf{B}_i^{\frac{1}{2}} \log \left(\mathbf{B}_i^{-\frac{1}{2}} \mathbf{B}_{i-1} \mathbf{B}_i^{-\frac{1}{2}} \right) \mathbf{B}_i^{\frac{1}{2}} \\ R_{\mathbf{V}_i}^{-1}(\mathbf{V}_{i-1}) &= \mathbf{V}_{i-1} - \mathbf{V}_i \end{aligned}$$

where \log is the matrix logarithm operator. The predicted solution is then obtained by taking a step s_t and performing a backtracking line search in the direction $-\hat{\xi}$ i.e.,

$$(\hat{\mathbf{U}}_{i+1}, \hat{\mathbf{B}}_{i+1}, \hat{\mathbf{V}}_{i+1}) = R_{(\mathbf{U}_i, \mathbf{B}_i, \mathbf{V}_i)}(-s_t \hat{\xi}). \quad (21)$$

A good choice of the initial step size s_t is $\frac{\lambda_{j+1} - \lambda_j}{\lambda_j - \lambda_{j-1}}$. The motivation for the choice comes from the observation that it is optimal when the solution path is a straight line in the Euclidean space. The numerical complexity to perform the prediction step in the manifold $\overline{\mathcal{M}}_p$ is $O(np^2 + mp^2 + p^3)$.

6 Numerical Experiments

The overall optimization scheme with *descent-restart* and trust-region algorithm is denoted as “Descent-restart + TR” (TR). We test the proposed optimization framework on the problems of low-rank matrix completion and multivariate linear regression where trace norm penalization has shown efficient recovery. Full regularization paths are constructed with optimality certificates. All simulations in this section are performed in MATLAB on a 2.53 GHz Intel Core i5 machine with 4 GB of RAM.

6.1 Diagonal versus matrix scaling

Before entering a detailed numerical experiment we illustrate here the empirical evidence that constraining \mathbf{B} to be diagonal (as is the case with SVD) is detrimental to optimization. To this end, we consider the simplest implementation of a gradient descent algorithm for matrix completion problem (see below). The plots shown in Figure 3 compare the behavior of the same algorithm in the search space $\text{St}(p, n) \times S_{++}(p) \times \text{St}(p, m)$ (polar factorization) and $\text{St}(p, n) \times \text{Diag}_+(p) \times \text{St}(p, m)$ (SVD). $\text{Diag}_+(p)$ is the set of diagonal matrices with positive entries. The empirical observation that convergence suffers from imposing diagonalization on \mathbf{B} is a generic observation that doesn’t depend on the particular problem at hand. The problem here involves completing a 200×200 of rank 5 from 40% of observed entries. λ is fixed at 10^{-10} .

6.2 Low-rank matrix completion

The problem of matrix completion involves completing an $n \times m$ matrix when only a few entries of the matrix are known. Presented in this way the problem is “ill-posed” but becomes considerably interesting when in addition a *low-rank reconstruction* is also sought. Given an incomplete low-rank (but unknown) $n \times m$ real matrix $\tilde{\mathbf{X}}$, a convex relaxation of the matrix completion problem is

$$\min_{\mathbf{X} \in \mathbb{R}^{n \times m}} \|\mathbf{W} \odot (\tilde{\mathbf{X}} - \mathbf{X})\|_F^2 + \lambda \|\mathbf{X}\|_* \quad (22)$$

for $\mathbf{X} \in \mathbb{R}^{n \times m}$ and a regularization parameter λ . Here $\|\cdot\|_F$ denotes the Frobenius norm, matrix \mathbf{W} is an $n \times m$ *weight* matrix with binary entries and the operator \odot denotes element-

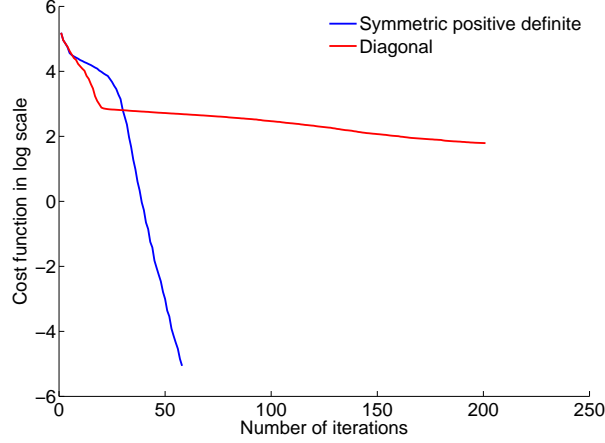


Figure 3: Convergence of a gradient descent algorithm is affected by making \mathbf{B} diagonal.

wise multiplication. If \mathcal{X} is the set of known entries (i, j) in $\tilde{\mathbf{X}}$ then,

$$\mathbf{W}_{ij} = \begin{cases} 1 & \text{if } (i, j) \in \mathcal{X}, \\ 0 & \text{otherwise.} \end{cases}$$

The problem of matrix completion is known to be combinatorially hard. However, by solving the convex relaxation (22) a low-rank reconstruction is possible with a very high probability [13, 18] under certain assumptions on the number of observed entries. For an exact reconstruction, the lower bound on the number of known entries is typically of the order $O(nr + mr)$ where r is the rank of the optimal solution. Consequently, it leads to a very sparse weight matrix \mathbf{W} , which plays a very crucial role for efficient algorithmic implementations. For our case, we assume that the lower bound on the number of entries is met and we seek a solution to the optimization problem (22). Customizing the terminology for the present problem, the convex function is

$$f(\mathbf{X}) = \|\mathbf{W} \odot (\tilde{\mathbf{X}} - \mathbf{X})\|_F^2.$$

Using the factorization $\mathbf{X} = \mathbf{UBV}^T$, the p -ranked formulation is

$$\bar{\phi}(\mathbf{U}, \mathbf{B}, \mathbf{V}) = \|\mathbf{W} \odot (\tilde{\mathbf{X}} - \mathbf{UBV}^T)\|_F^2 + \lambda \text{Trace}(\mathbf{B})$$

where $(\mathbf{U}, \mathbf{B}, \mathbf{V}) \in \overline{\mathcal{M}}_p$. The dual variable $\mathbf{S} = 2(\mathbf{W} \odot (\mathbf{UBV}^T - \tilde{\mathbf{X}}))$. The gradient of $\bar{\phi}$ in \mathcal{E} can be computed as

$$\text{Grad}_{\mathbf{U}} \bar{\phi} = \mathbf{SVB}, \quad \text{Grad}_{\mathbf{B}} \bar{\phi} = \mathbf{U}^T \mathbf{SV} + \lambda \mathbf{I} \quad \text{and} \quad \text{Grad}_{\mathbf{V}} \bar{\phi} = \mathbf{S}^T \mathbf{UB}.$$

The directional derivative of the gradient of $\bar{\phi}$ along $\mathbf{Z} = (\mathbf{Z}_{\mathbf{U}}, \mathbf{Z}_{\mathbf{B}}, \mathbf{Z}_{\mathbf{V}}) \in \mathcal{E}$ in the space \mathcal{E} is

$$\begin{pmatrix} \mathbf{SVZ}_{\mathbf{B}} + \mathbf{SZ}_{\mathbf{V}}\mathbf{B} + \mathbf{S}_* \mathbf{VB}, & \mathbf{Z}_{\mathbf{U}}^T \mathbf{SV} + \mathbf{USZ}_{\mathbf{V}} + \mathbf{U}^T \mathbf{S}_* \mathbf{V}, \\ \mathbf{S}^T \mathbf{UZ}_{\mathbf{B}} + \mathbf{S}^T \mathbf{Z}_{\mathbf{U}} \mathbf{B} + \mathbf{S}_*^T \mathbf{UB}, & \end{pmatrix}$$

where $\mathbf{S}_* = \text{D}_{(\mathbf{U}, \mathbf{B}, \mathbf{V})} \mathbf{S}[\mathbf{Z}] = 2(\mathbf{W} \odot (\mathbf{Z}_{\mathbf{U}} \mathbf{B} \mathbf{V}^T + \mathbf{UZ}_{\mathbf{B}} \mathbf{V}^T + \mathbf{UBZ}_{\mathbf{V}}^T))$ is the directional derivative of \mathbf{S} along \mathbf{Z} . The Riemannian gradient and Hessian are computed using formulae developed

in Section 3. Note that since \mathbf{W} is sparse, \mathbf{S} and \mathbf{S}_* are sparse too. As a consequence, the numerical complexity of evaluating objects needed in the trust-region algorithm is of order $O(|\mathcal{X}|p + np^2 + mp^2 + p^3)$ where $|\mathcal{X}|$ is the number of known entries. Asymptotically, the total (problem dependent and manifold related) numerical complexity per iteration for solving the problem (2) using the trust-region algorithm proposed earlier is of order $O(|\mathcal{X}|p)$. For using the optimization scheme described in Table 1, an additional *thin* singular value decomposition of dual variable \mathbf{S} is performed. Due to sparsity in \mathbf{S} , it can be computed with numerical complexity of order $O(|\mathcal{X}|)$. The linear complexity with respect to the number of known entries allows us to handle potentially very large datasets.

Fenchel dual and duality gap for matrix completion

For the matrix completion problem, the sampling operation is the linear operator $\mathcal{A}(\mathbf{X}) = \mathbf{W} \odot \mathbf{X}$. We can, therefore, define a new function ψ such that $f(\mathbf{X}) = \psi(\mathbf{W} \odot \mathbf{X})$. The dual candidate \mathbf{M} is defined by

$$\mathbf{M} = \min\left(1, \frac{\lambda}{\sigma_\psi}\right) \text{Grad}\psi$$

where $\text{Grad}\psi(\mathbf{W} \odot \mathbf{X}) = 2(\mathbf{W} \odot \mathbf{X} - \mathbf{W} \odot \tilde{\mathbf{X}})$ and σ_ψ is the dominant singular value of $\mathcal{A}^*(\text{Grad}\psi)$ (refer Section 2.2 for details). In matrix form, $\mathcal{A}^*(\text{Grad}\psi)$ can be written as $\mathbf{W} \odot \text{Grad}\psi$. Finally, the Fenchel dual ψ^* at a dual candidate \mathbf{M} can be computed as

$$\psi^*(\mathbf{M}) = \sup_{\mathbf{Z} \in \mathbb{R}^{n \times m}} \text{Trace}(\mathbf{M}^T \mathbf{Z}) - \|\mathbf{W} \odot \tilde{\mathbf{X}} - \mathbf{Z}\|_F^2 \quad (23)$$

where \mathbf{Z} is in the domain of ψ . The maximum of (23) is obtained at

$$\mathbf{Z}^* = \frac{1}{2}(\mathbf{M} + 2\mathbf{W} \odot \tilde{\mathbf{X}})$$

and so,

$$\begin{aligned} \psi^*(\mathbf{M}) &= \text{Trace}(\mathbf{M}^T \mathbf{Z}) - \|\mathbf{W} \odot \tilde{\mathbf{X}} - \mathbf{Z}\|_F^2 \\ &= \text{Trace}(\mathbf{M}^T \mathbf{M})/4 + \text{Trace}(\mathbf{M}^T (\mathbf{W} \odot \tilde{\mathbf{X}})) \end{aligned}$$

The final expression for the duality gap at a point \mathbf{X} and a dual candidate $\mathbf{M} = \min(1, \frac{\lambda}{\sigma_\psi}) \text{Grad}\psi$ is

$$f(\mathbf{X}) + \lambda \|\mathbf{X}\|_* + \text{Trace}(\mathbf{M}^T \mathbf{M})/4 + \text{Trace}(\mathbf{M}^T (\mathbf{W} \odot \tilde{\mathbf{X}})). \quad (24)$$

In terms of the polar factorization $\mathbf{X} = \mathbf{UBV}^T$, the duality gap expression simplifies to

$$f(\mathbf{UBV}^T) + \lambda \text{Trace}(\mathbf{B}) + \text{Trace}(\mathbf{M}^T \mathbf{M})/4 + \text{Trace}(\mathbf{M}^T (\mathbf{W} \odot \tilde{\mathbf{X}})).$$

The above expression shows that the numerical cost to compute the duality gap is $O(|\mathcal{X}|)$ which makes the computation numerically tractable.

6.2.1 An example

A 100×100 random matrix of rank 10 is generated according to a Gaussian distribution with zero mean and unit standard deviation. 20% of the entries are randomly removed with uniform

probability. To reconstruct the original matrix we run the optimization scheme proposed in the Table 1 along with the trust-region algorithm to solve the non-convex problem. For illustration purposes λ is fixed at 1×10^{-5} . We also assume that we do not have any a priori knowledge of the optimal rank and, thus, start from rank 1. The trust-region algorithm stops when the relative or absolute variation of the cost function falls below 1×10^{-10} . The rank-incrementing strategy stops when relative duality gap is less than 1×10^{-5} , i.e.,

$$\frac{f(\mathbf{X}) + \lambda \|\mathbf{X}\|_* + \psi^*(\mathbf{M})}{|\psi^*(\mathbf{M})|} \leq 1 \times 10^{-5}$$

respectively. Convergence plots of the scheme are shown in Figure 4. A good way to charac-

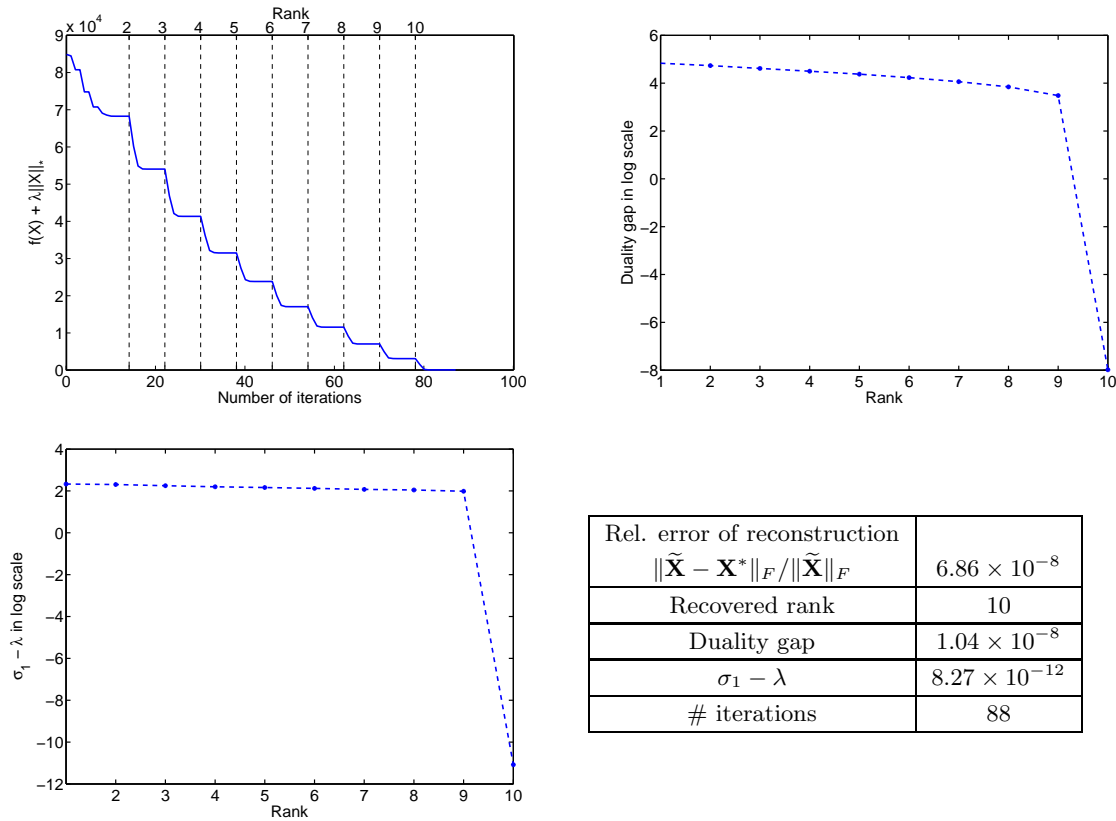


Figure 4: Matrix completion by trace norm minimization algorithm with $\lambda = 1 \times 10^{-5}$. Upper left: Rank incremental strategy with descent directions. Upper right: Optimality certificate of the solution with duality gap. Lower left: Convergence to the global solution according to Proposition 2.1 . Lower right: Recovery of the original low-rank matrix.

terize matrix reconstruction is to look at the relative error of reconstruction, defined as,

$$\text{Rel. error of reconstruction} = \|\tilde{\mathbf{X}} - \mathbf{X}^*\|_F / \|\tilde{\mathbf{X}}\|_F$$

where \mathbf{X}^* is the output of the trace norm minimization algorithm. Next, to understand low-rank matrix reconstruction by trace norm minimization we repeat the experiment for a number of values of λ all initialized from the same starting point and report the relative reconstruction error in Table 3 averaged over 5 runs. This, indeed, confirms that matrix reconstruction is possible by solving the trace norm minimization problem (22).

λ	10	10^{-2}	10^{-5}	10^{-8}
Rel. reconstruction error	6.33×10^{-2}	7.42×10^{-5}	7.11×10^{-8}	6.89×10^{-11}
Recovered rank	10	10	10	10

Table 3: Efficacy of trace norm penalization to reconstruct low-rank matrices by solving (22).

6.2.2 Regularization path for matrix completion

In order to compute the entire regularization path, we employ the predictor-corrector approach described in Table 2 to find solutions for a grid of λ values. For the purpose of illustration, a geometric sequence of λ values is created with the maximum value fixed at $\lambda_1 = 1 \times 10^3$, the minimum value is set at $\lambda_N = 1 \times 10^{-3}$ and a reduction factor $\gamma = 0.95$ such that $\lambda_{i+1} = \gamma\lambda_i$. Similar to the earlier example, a 100×100 matrix of rank 10 is generated under the standard assumptions. In this case we remove 20% of the entries with uniform probability. The algorithm for a $\lambda_i \in \{\lambda_1, \dots, \lambda_N\}$ stops when the relative duality gap falls below 1×10^{-5} . Various plots are shown in Figure 5. Figure 5 also demonstrates the advantage of the scheme in Table 2 with respect to a warm-restart approach. We compare both approaches on the basis of

$$\text{Inaccuracy in prediction} = \bar{\phi}(\hat{\mathbf{X}}(\lambda_i)) - \bar{\phi}(\mathbf{X}^*(\lambda_i)) \quad (25)$$

where $\mathbf{X}^*(\lambda_i)$ is the global solution at λ_i and $\hat{\mathbf{X}}(\lambda_i)$ is the predicted (or estimated) solution. A lower inaccuracy means better prediction. It should be emphasized that in Figure 4 most of the points on the curve of the objective function have no other utility than being intermediate iterates towards the global solution of the algorithm. In contrast all the points of the curve of optimal cost values in Figure 5 are now global minima for different values of λ .

6.2.3 Competing methods for matrix completion

In this section, we analyze the following state-of-the-art algorithms for low-rank matrix completion, namely,

1. SVT algorithm by Cai et al. [12]
2. FPCA algorithm by Ma et al. [20]
3. SOFT-IMPUTE (Soft-I) algorithm by Mazumder et al. [21]

While FPCA and SOFT-IMPUTE solve (22), the iterates of SVT converge towards a solution of the optimization problem

$$\begin{aligned} \min \quad & \tau \|\mathbf{X}\|_* + \frac{1}{2} \|\mathbf{X}\|_F^2 \\ \text{subject to} \quad & \mathbf{W} \odot \mathbf{X} = \mathbf{W} \odot \tilde{\mathbf{X}} \end{aligned}$$

where τ is a regularization parameter. For simulation studies we use the MATLAB codes supplied on the authors' webpages for SVT and FPCA. Due to simplicity of the SOFT-IMPUTE algorithm we use our own MATLAB implementation. The numerically expensive step in all

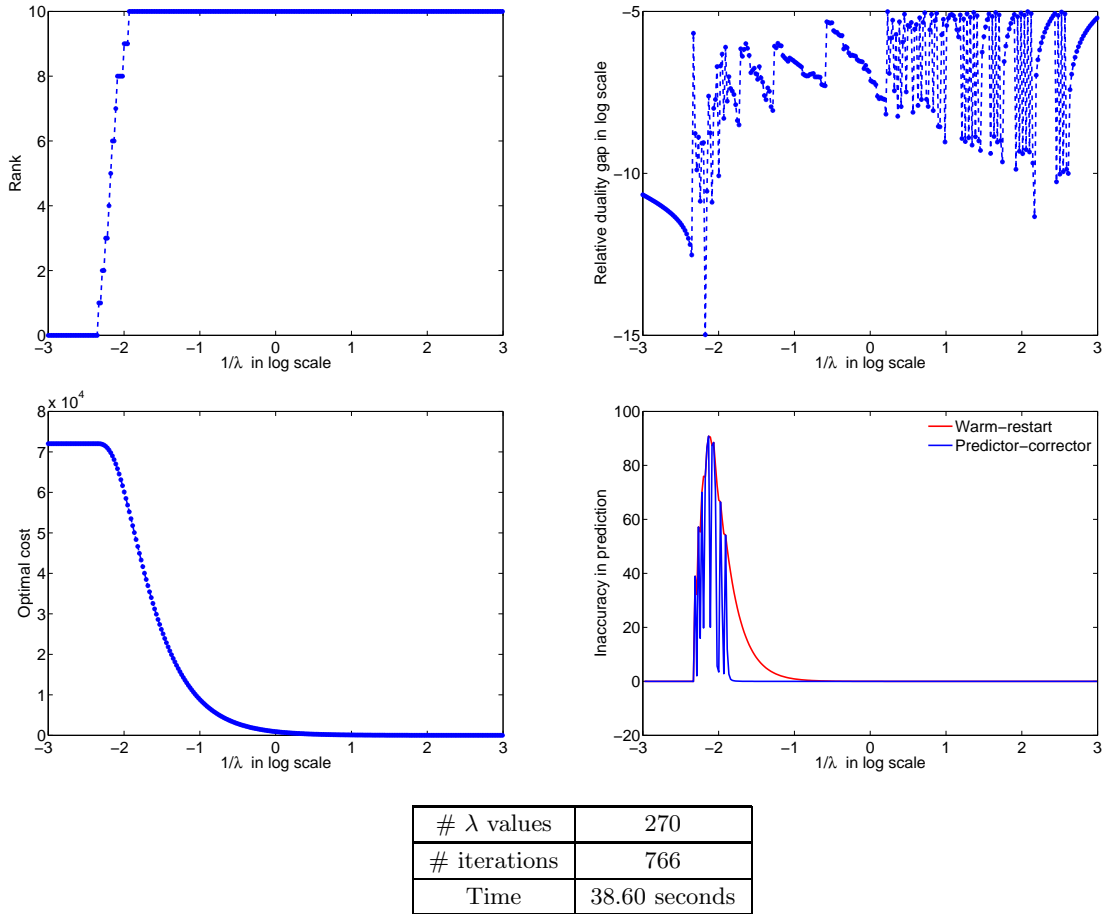


Figure 5: Computation of entire regularization path using Descent-restart + TR with a predictor-corrector approach. Upper left: Recovery of all ranks optimal solutions. Upper right: Optimality certificate for the regularization path. Lower left: Path traced by the algorithm. Lower right: Better prediction by the algorithm in Table 2 than a pure warm-restart approach. Table: Number of iterations per value of λ is < 3 .

these algorithms is the computation of the *singular value thresholding* operation. To reduce the computational burden FPCA uses a linear time approximate singular value decomposition (SVD). Similarly, the authors of SVT and SOFT-IMPUTE implement the thresholding operation by utilizing the *sparse + low-rank* structure of the iterates. Specifically, SVT and SOFT-IMPUTE use PROPACK which exploit sparsity of the data while computing singular values [19]. It should be emphasized that the performance of SOFT-IMPUTE greatly varies with the singular values computation at each iteration. For our simulations we compute 20 dominant singular values at each iteration of SOFT-IMPUTE.

Convergence behavior with varying λ

In this section we analyze the algorithms FPCA, SOFT-IMPUTE and Descent-restart + TR in terms of their ability to solve (22) as λ is varied. SVT is not used for this test since it optimizes a different cost function. We plot the objective function $f(\mathbf{X}) + \lambda\|\mathbf{X}\|_*$ against the

number of iterations for a number of λ values.

We generate a 100×100 random matrix of rank 8 under standard assumptions. 80% of the entries are observed. The algorithms Descent-restart + TR, FPCA and SOFT-IMPUTE are initialized from the same point. The algorithms are stopped when either the variation or relative variation of $f(\mathbf{X}) + \lambda \|\mathbf{X}\|_*$ is less than 1×10^{-10} . The maximum number of iterations is set at 500. The rank incrementing procedure of our algorithm is stopped when the relative duality gap falls below 1×10^{-5} .

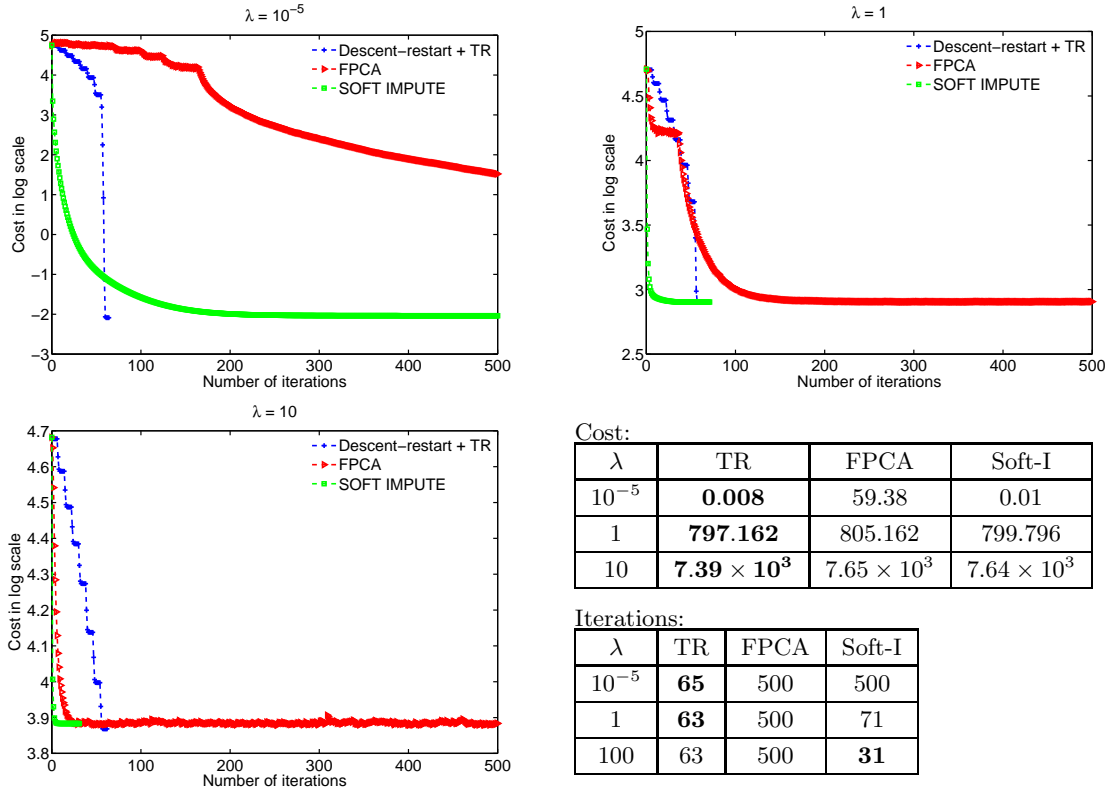


Figure 6: Convergence behavior of different algorithms with different λ values.

The plots are shown in Figure 6. Descent-restart + TR outperforms the others in terms of accuracy of solutions obtained with minimal number of iterations. The convergence behavior of FPCA is greatly affected by λ . It has a slow convergence for a small λ while for a larger λ , the algorithm fluctuates. SOFT-IMPUTE has a nice convergence in all the three cases, however, the convergence suffers when a more accurate solution is sought.

Convergence test

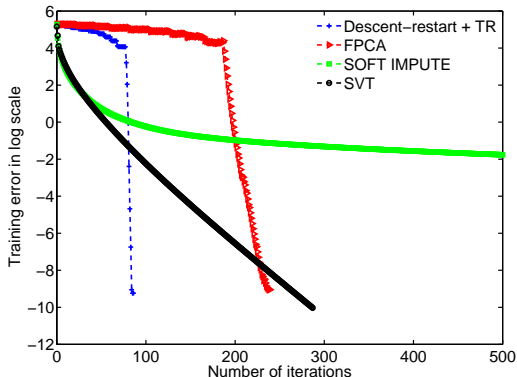
To understand the convergence behavior of different algorithms involving different optimization problems, we look at the evolution of the training error [12, 21] defined as

$$\text{Training error} = \|\mathbf{W} \odot (\tilde{\mathbf{X}} - \mathbf{X})\|_F^2,$$

with iterations. We generate a 150×300 random matrix of rank 10 under standard assumptions. Only 50% of the entries are observed. The algorithms Descent-restart + TR, FPCA

and SOFT-IMPUTE (Soft-I) are initialized from the same iterate with a fixed λ . We fix $\lambda = 1 \times 10^{-5}$ as it gives a good reconstruction to compare algorithms. For SVT we use the initialization including $\tau = 5\sqrt{nm}$ and a step size of $\frac{1.2}{f}$ as suggested in the paper [12] where f is the fraction of known entries. The algorithms are stopped when the variation or relative variation of Training error is less than 1×10^{-10} . The maximum number of iterations is set at 500. The rank incrementing procedure of our algorithm is stopped when either the duality gap falls below 1×10^{-3} or the relative duality gap falls below 1×10^{-5} .

SOFT-IMPUTE initially has a very fast convergence (for iterations less than 60) but the performance slows down later. Consequently, it exceeds the maximum limit of iterations. Descent-restart + TR, SVT and FPCA, on the other hand, seem to be better equipped for targeting more accurate solutions. Descent-restart + TR takes the smallest number of iterations of all.



	# iterations	Time in secs
TR	87	6.25
FPCA	239	2.47
SVT	288	16.8
Soft-I	500	13.79

Figure 7: Convergence behavior of different algorithms in terms of minimizing Training error. Left: Faster convergence of Descent-restart and FPCA. Table: Timings and number of iterations averaged over 5 runs.

Scaling test

To analyze the scalability of these algorithms to larger problems we perform a test where we vary the problem size n from 200 to 2200. For each n , we generate a random matrix of size $n \times n$ of rank 10 under standard assumptions. Each entry is observed with uniform probability of $f = \frac{4r \log_{10}(n)}{n}$ [18]. The initializations are chosen as in the earlier example. We note the time and number of iterations taken by the algorithms until a stopping criterion is satisfied or when the number of iterations exceed 500. The stopping criterion is same as the one used before for comparison. Results averaged over 5 runs are shown in Figure 8.

Comments on matrix completion algorithms

We summarize our observations in the following points.

- The convergence rate of SOFT-IMPUTE is greatly dependent on the computation of singular values. For large scale problems this is a bottleneck and the performance is

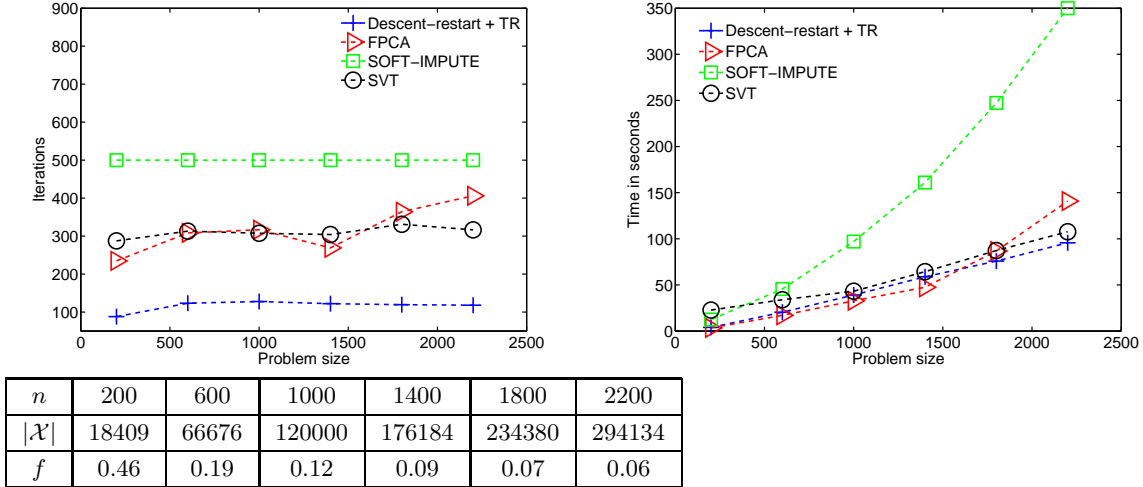


Figure 8: Analysis of the algorithms on randomly generated datasets of rank 10 with varying fractions of missing entries. The reduced performance of SOFT-IMPUTE is due to its slower convergence. SVT, FPCA and Descent-restart + TR have similar performances but Descent-restart + TR usually outperforms others.

greatly affected. However, in our experiments, it performs quite well within a reasonable accuracy as seen in Figure 6 and Figure 7.

- SVT, in general, performs quite well on random examples. The choice of the fixed step size and regularization parameter τ , however, affect the convergence speed of the algorithm [20, 21].
- FPCA has a superior numerical complexity per iteration owing to an approximate singular value decomposition [20]. But the performance suffers as the regularization parameter λ is increased as shown in Figure 6.
- In all the simulation studies on random examples Descent-restart+TR has shown better performance than others on different benchmarks and it competes effectively with the state-of-the-art.

6.3 Multivariate linear regression

Given matrices $\mathbf{Y} \in \mathbb{R}^{n \times k}$ (response space) and $\mathbf{X} \in \mathbb{R}^{n \times q}$ (input data space), we seek to learn a weight/coefficient matrix $\mathbf{W} \in \mathbb{R}^{q \times k}$ that minimizes the *loss* between \mathbf{Y} and \mathbf{XW} [37]. Here n is the number of observations, q is the number of predictors and k is the number of responses. One popular approach to multivariate linear regression problem is by minimizing a *quadratic loss* function. Note that in various applications *responses* are related and may therefore, be represented with much fewer coefficients. From an optimization point to view this corresponds to finding a low-rank coefficient matrix. The papers [37, 4], thus, motivate the use of trace norm regularization in the following optimization problem formulation, defined as,

$$\min_{\mathbf{W} \in \mathbb{R}^{q \times k}} \|\mathbf{Y} - \mathbf{XW}\|_F^2 + \lambda \|\mathbf{W}\|_*.$$

(Optimization variable is \mathbf{W} .) Although the focus here is on the quadratic loss function, the framework can be applied to other smooth loss functions as well. Other than the difference in the dual variable \mathbf{S} and \mathbf{S}_* , the rest of the computation of gradient and its directional derivative in the Euclidean space is similar to that of the low-rank matrix completion case.

$$\begin{aligned}\mathbf{S} &= 2(\mathbf{X}^T \mathbf{X} \mathbf{W} - \mathbf{X}^T \mathbf{Y}) \quad \text{and} \\ \mathbf{S}_* &= \text{D}_{(\mathbf{U}, \mathbf{B}, \mathbf{V})} \mathbf{S}[\mathbf{Z}] = 2(\mathbf{X}^T \mathbf{X} (\mathbf{Z}_{\mathbf{U}} \mathbf{B} \mathbf{V}^T + \mathbf{U} \mathbf{Z}_{\mathbf{B}} \mathbf{V}^T + \mathbf{U} \mathbf{B} \mathbf{Z}_{\mathbf{V}}^T))\end{aligned}$$

where $\mathbf{W} = \mathbf{U} \mathbf{B} \mathbf{V}^T$.

The numerical complexity per iteration is dominated by the numerical cost to compute $\bar{\phi}(\mathbf{U}, \mathbf{B}, \mathbf{V})$, \mathbf{S} and terms like $\mathbf{S} \mathbf{V} \mathbf{B}$. The cost of computing $\bar{\phi}$ is of $O(nqp + nkp + kp^2 + nk)$ and $\mathbf{S} \mathbf{V} \mathbf{B}$ is $O(q^2p + qkp + kp^2)$. And that of full matrix \mathbf{S} is $O(q^2p + qkp + kp^2)$. From a *cubic* numerical complexity of $O(q^2k)$ per iteration (using the full matrix \mathbf{W}) the low-rank factorization reduces the numerical complexity to $O(q^2p + qkp)$ which is *quadratic*. Note that the numerical complexity per iteration is linear in n .

Fenchel dual and duality gap for multivariate linear regression

For the multivariate linear regression problem $\mathcal{A}(\mathbf{W}) = \mathbf{X} \mathbf{W}$ and therefore, we can define ψ such that $f(\mathbf{W}) = \psi(\mathbf{X} \mathbf{W})$. So, $\mathcal{A}^*(\eta) = \mathbf{X}^T \eta$. The dual candidate \mathbf{M} is defined by

$$\mathbf{M} = \min\left(1, \frac{\lambda}{\sigma_\psi}\right) \text{Grad} \psi$$

where $\text{Grad} \psi(\mathbf{X} \mathbf{W}) = 2(\mathbf{X} \mathbf{W} - \mathbf{Y})$ and σ_ψ is the dominant singular value of $\mathcal{A}^*(\text{Grad} \psi) = \mathbf{X}^T \text{Grad} \psi$. The Fenchel dual ψ^* (after few more steps) can be computed as

$$\psi^*(\mathbf{M}) = \text{Trace}(\mathbf{M}^T \mathbf{M})/4 + \text{Trace}(\mathbf{M}^T \mathbf{Y}).$$

Finally, the duality gap is computed as $f(\mathbf{W}) + \lambda \|\mathbf{W}\|_* + \psi^*(\mathbf{M})$. As we use a low-rank factorization of \mathbf{W} , i.e., $\mathbf{W} = \mathbf{U} \mathbf{B} \mathbf{V}^T$ the numerical complexity of finding the duality gap is dominated by numerical cost of computing $\psi^*(\mathbf{M})$ which is also of the order of the cost of computing $\bar{\phi}(\mathbf{U}, \mathbf{B}, \mathbf{V})$.

- $\mathbf{M} \rightarrow$ order $O(nqp + nkp + kp^2)$
- $\psi^*(\mathbf{M}) \rightarrow$ order $O(nk)$.

6.3.1 Regularization path for multivariate linear regression

An input data matrix \mathbf{X} of size 5000×120 is randomly generated according to a Gaussian distribution with zero mean and unit standard deviation. The response matrix \mathbf{Y} is computed as $\mathbf{X} \mathbf{W}_*$ where \mathbf{W}_* is a randomly generated coefficient matrix of rank 5 matrix and size 120×100 . We randomly split the observations as well as responses into *training* and *testing* datasets in the ratio 70/30 resulting in $\mathbf{Y}_{\text{train}}/\mathbf{Y}_{\text{test}}$ and $\mathbf{X}_{\text{train}}/\mathbf{X}_{\text{test}}$. A Gaussian white noise of zero mean and variance σ_{noise}^2 is added to the training response matrix $\mathbf{Y}_{\text{train}}$ resulting in $\mathbf{Y}_{\text{noise}}$. We learn the coefficient matrix \mathbf{W} by minimizing the *scaled* cost function, i.e.,

$$\min_{\mathbf{W} \in \mathbb{R}^{q \times k}} \frac{1}{nk} \|\mathbf{Y}_{\text{noise}} - \mathbf{X}_{\text{train}} \mathbf{W}\|_F^2 + \lambda \|\mathbf{W}\|_*,$$

where λ is a regularization parameter. We validate the learning by computing the root mean square error (rmse) defined as

$$\text{Test rmse} = \sqrt{\frac{1}{n_{\text{test}}k} \|\mathbf{Y}_{\text{test}} - \mathbf{X}_{\text{test}} \mathbf{W}\|_F^2}$$

where n_{test} is the number of test observations. Similarly, the signal to noise ratio (SNR) is defined as $\sqrt{\frac{\|\mathbf{Y}_{\text{train}}\|_F^2}{\sigma_{\text{noise}}^2}}$.

We compute the entire regularization path for four different SNR values. The maximum value of λ is fixed at 10 and the minimum value is set at 1×10^{-5} with the reduction factor $\gamma = 0.95$. Apart from this we also put the restriction that we only fit ranks less than 30. The solution to an optimization problem for λ_j is claimed to have been obtained when either the duality gap falls below 1×10^{-2} or the relative duality gap falls below 1×10^{-2} or $\sigma_1 - \lambda$ is less than 1×10^{-2} . Similarly, the trust-region algorithm stops when relative or absolute variation of the cost function falls below 1×10^{-10} . The results are summarized in Figure 9.

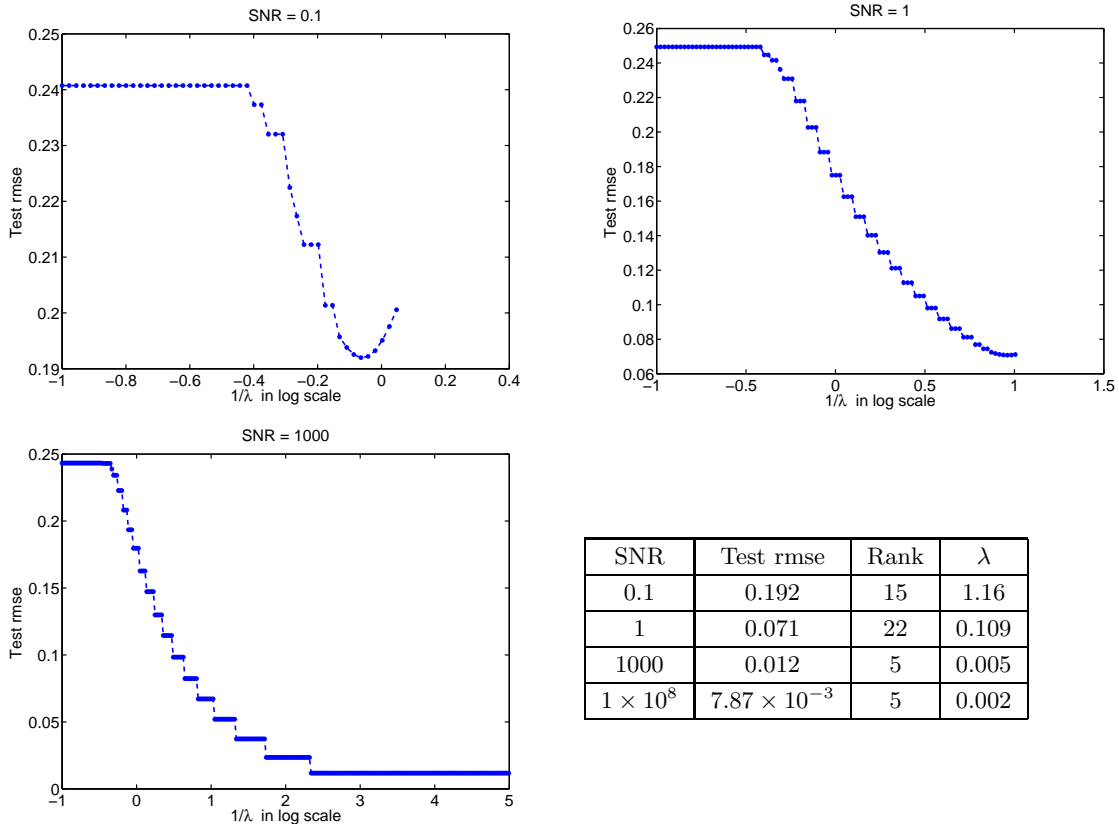


Figure 9: Regularization path for multivariate linear regression with various SNR values. Results are averaged over 5 random 70/30 splits.

7 Conclusion

Three main ideas have been presented in this paper. First, we have given a framework to solve a general trace norm minimization problem (1) with a sequence of increasing but fixed-

rank non-convex problems (2). We have analyzed the convergence criterion and duality gap which are used to monitor convergence to a solution of the original problem. The duality gap expression was shown numerically tractable even for large problems thanks to the specific choice of the low-rank parametrization. We have also given a way of incrementing the rank while simultaneously ensuring a decrease of the cost function. This may be termed as a *descent-restart* approach. The second contribution of the paper is to present a second-order trust-region algorithm for a general p – rank (fixed-rank) optimization in the quotient search space $\text{St}(p, n) \times S_{++}(p) \times \text{St}(p, m) / \mathcal{O}(p)$ equipped with the natural metric \bar{g} (11). The search space with the metric \bar{g} has the structure of a Riemannian submersion [3]. We have used manifold-optimization techniques [3] to derive the required geometric objects in order to devise a second-order algorithm. With a proper parameter tuning the proposed trust-region algorithm guarantees a quadratic rate of convergence. The third contribution of the paper is to develop a predictor-corrector algorithm on the quotient manifold where the predictor step is along the first-order approximation of the geodesic. The corrector step is achieved by initializing the descent-restart approach from the predicted point. The resulting performance is superior to the warm-restart approach.

These ideas have been applied to the problems of low-rank matrix completion and multivariate linear regression leading to encouraging numerical results.

References

- [1] P.-A. ABSIL, C. G. BAKER, AND K. A. GALLIVAN, *Trust-region methods on Riemannian manifolds*, Foundations of Computational Mathematics, 7 (2007), pp. 303–330.
- [2] P.-A. ABSIL, M. ISHTEVA, L. DE LATHAUWER, AND S. VAN HUFFEL, *A geometric Newton method for Oja’s vector field*, Neural Computation, 21 (2009), pp. 1415–1433.
- [3] P.-A. ABSIL, R. MAHONY, AND R. SEPULCHRE, *Optimization Algorithms on Matrix Manifolds*, Princeton University Press, 2008.
- [4] Y. AMIT, M. FINK, N. SREBRO, AND S. ULLMAN, *Uncovering shared structures in multiclass classification*, in ICML, Z. Ghahramani, ed., vol. 227 of ACM International Conference Proceeding Series, ACM, 2007, pp. 17–24.
- [5] F. BACH, *Consistency of trace norm minimization*, Journal of Machine Learning Research, 9 (2008), pp. 1019–1048.
- [6] F. BACH, R. JENATTON, J. MAIRAL, AND G. OBOZINSKY, *Convex optimization with sparsity-inducing norms*, In S. Sra, S. Nowozin, S. J. Wright., editors, Optimization for Machine Learning, MIT Press (To appear), 2011.
- [7] S. BONNABEL AND R. SEPULCHRE, *Geometric distance and mean for positive semi-definite matrices of fixed rank*, SIAM J. Matrix Anal. Appl., 31 (2009), pp. 1055–1070.

- [8] N. BOUMAL AND P.-A. ABSIL, *Rtrmc: A Riemannian trust-region method for low-rank matrix completion*, in Proceedings of the Neural Information Processing Systems Conference, NIPS, 2011.
- [9] S. BOYD AND L. VANDENBERGHE, *Convex optimization*, Cambridge University Press, March 2004.
- [10] M. BRAND, *Fast low-rank modifications of the thin singular value decomposition*, Linear Algebra and Its Applications, 415 (2006), pp. 20–30.
- [11] S. BURER AND R. D. C. MONTEIRO, *A nonlinear programming algorithm for solving semidefinite programs via low-rank factorization*, Mathematical Programming, 95 (2003), pp. 329–357.
- [12] J.-F. CAI, E. J. CANDÈS, AND Z. SHEN, *A singular value thresholding algorithm for matrix completion*, SIAM Journal On Optimization, 20 (2010), pp. 1956–1982.
- [13] E. J. CANDÈS AND B. RECHT, *Exact matrix completion via convex optimization*, Foundations of Computational Mathematics, 9 (2009), pp. 717–772.
- [14] A. EDELMAN, T. A. ARIAS, AND S. T. SMITH, *The geometry of algorithms with orthogonality constraints*, SIAM Journal On Matrix Analysis and Applications, 20 (1998), pp. 303–353.
- [15] M. FAZEL, *Matrix Rank Minimization with Applications*, PhD thesis, Stanford University, 2002.
- [16] M. JOURNÉE, *Geometric algorithms for component analysis with a view to gene expression data analysis*, PhD thesis, University of Liège, Liège, Belgium, 2009.
- [17] M. JOURNÉE, F. BACH, P.-A. ABSIL, AND R. SEPULCHRE, *Low-rank optimization on the cone of positive semidefinite matrices*, SIAM Journal on Optimization, 20 (2010), pp. 2327–2351.
- [18] R. H. KESHAVAN AND S. OH, *A gradient descent algorithm on the Grassman manifold for matrix completion*, CoRR, abs/0910.5260 (2009).
- [19] R. M. LARSEN, *PROPACK - software for large and sparse svd calculations*.
- [20] S. MA, D. GOLDFARB, AND L. CHEN, *Fixed point and bregman iterative methods for matrix rank minimization*, Math. Program., 128 (2011), pp. 321–353.
- [21] R. MAZUMDER, T. HASTIE, AND R. TIBSHIRANI, *Spectral regularization algorithms for learning large incomplete matrices*, Journal of Machine Learning Research, 11 (2010), pp. 2287–2322.
- [22] R. MEKA, P. JAIN, AND I. S. DHILLON, *Guaranteed rank minimization via singular value projection*, CoRR, abs/0909.5457 (2009).

- [23] G. MEYER, *Geometric optimization algorithms for linear regression on fixed-rank matrices*, PhD thesis, University of Liège, 2011.
- [24] G. MEYER, S. BONNABEL, AND R. SEPULCHRE, *Regression on fixed-rank positive semidefinite matrices: a riemannian approach*, Journal of Machine Learning Research, 12 (Feb) (2010).
- [25] ———, *Linear regression under fixed-rank constraints: a Riemannian approach*, in Proceedings of the 28th International Conference on Machine Learning (ICML 2011), 2011.
- [26] B. MISHRA, G. MEYER, AND R. SEPULCHRE, *Low-rank optimization for distance matrix completion*, in Proceedings of the 50th IEEE Conference on Decision and Control, 2011.
- [27] J. NOCEDAL AND S. J. WRIGHT, *Numerical Optimization*, Springer, New York, 2nd ed., 2006.
- [28] M.-Y. PARK AND T. HASTIE, *Regularization path algorithms for detecting gene interactions*, tech. rep., Department of Statistics, Stanford University, 2006.
- [29] B. RECHT, M. FAZEL, AND P. A. PARRILO, *Guaranteed minimum-rank solutions of linear matrix equations via nuclear norm minimization*, SIAM Review, 52 (2010), pp. 471–501.
- [30] L. SIMONSSON AND L. ELDÉN, *Grassmann algorithms for low rank approximation of matrices with missing values*, BIT Numerical Mathematics, 50 (2010), pp. 173–191.
- [31] S. T. SMITH, *Covariance, subspace, and intrinsic Cramér-Rao bounds*, IEEE Transactions on Signal Processing, 53 (2005), pp. 1610–1630.
- [32] N. SREBRO AND T. JAAKKOLA, *Weighted low-rank approximations*, in Proceedings of the 20th International Conference on Machine Learning (ICML), 2003, pp. 720–727.
- [33] K. C. TOH AND S. YUN, *An accelerated proximal gradient algorithm for nuclear norm regularized least squares problems*, Pacific Journal of Optimization, 6 (2010).
- [34] B. VANDEREYCKEN, *Low-rank matrix completion by Riemannian optimization*, tech. rep., Mathematics Institute of Computational Science and Engineering, EPFL, 2011.
- [35] M. VOUNOU, T. E. NICHOLS, G. MONTANA, AND ALZHEIMER’S DISEASE NEUROIMAGING INITIATIVE, *Discovering genetic associations with high-dimensional neuroimaging phenotypes: A sparse reduced-rank regression approach*, Neuroimage, 53 (2010), pp. 1147–59.
- [36] Z. WEN, W. YIN, AND Y. ZHANG, *Solving a low-rank factorization model for matrix completion by a nonlinear successive over-relaxation algorithm*, Tech. Rep. TR10-07, CAAM, Rice University, 2010.

- [37] M. YUAN, A. EKICI, Z. LU, AND R. D. C. MONTEIRO, *Dimension reduction and coefficient estimation in multivariate linear regression*, Journal of the Royal Statistical Society, Series B 69 (2007).